

## Ciprofloxacin adsorption on a mesoporous carbon prepared by a dual-template route

Na Ren<sup>a</sup>, Conghui Wang<sup>a</sup>, Wei Wei<sup>a,\*</sup>, Jiajia Li<sup>a</sup>, Xiaoqi Yue<sup>a</sup>, Guotong Qin<sup>b</sup>

<sup>a</sup>College of Biochemical Engineering, Beijing Union University, 18 Sanqu, Fatouxili, Beijing 100023, China, Tel./Fax: +86 10 52072157; emails: wlweiwei@buu.edu.cn (W. Wei), 171083210408@buu.edu.cn (N. Ren), 181083210407@buu.edu.cn (C. Wang), 458445925@qq.com (J. Li), xiaoqi\_yue@outlook.com (X. Yue)

<sup>b</sup>School of Space and Environment, Beihang University, No.9, Shahe Gaojiaoyuan South 3rd Street, Beijing 102206, China, email: qingt@buaa.edu.cn (G. Qin)

Received 11 August 2019; Accepted 28 February 2020

### ABSTRACT

Mesoporous carbon with a high specific surface area (1,342.8 m<sup>2</sup>/g) and a high mesopore volume (1.396 cm<sup>3</sup>/g) was prepared from Novalac phenol–formaldehyde resin as a carbon source, with F127 and nanosized silica as templates, followed by carbonization at high temperature. For comparison, other mesoporous carbon materials were prepared with only one template. The application of these mesoporous carbon materials and a commercial activated carbon for ciprofloxacin (CIP) removal from aqueous solution was investigated. At a low CIP concentration, the maximum adsorption of CIP on the mesoporous carbon was as high as 243.91 mg/g, which was the largest among these carbon materials and higher than that in literature. The adsorption capacities of these carbon adsorbents increased with an increase in mesopore volume. The equilibrium adsorption data were well described by the Langmuir isotherm. The adsorption kinetics followed a pseudo-second-order kinetic model. The effect of pH on the CIP adsorption was studied to investigate the adsorption mechanism.

*Keywords:* Mesoporous carbon; Double-template; Ciprofloxacin removal; Wastewater treatment; Adsorption modeling

### 1. Introduction

Ciprofloxacin (CIP) release into the aquatic environment constitutes an environmental problem because it induces bacterial drug resistance. Water resource pollution from CIP disposal has been a cause for concern recently. Many possible methods exist for CIP removal from wastewater. The adsorption technique is most suitable, because of its simplicity of operation and regeneration. Various adsorbents have been used, including kaolinite [1,2], activated carbon (AC) [3], montmorillonite [4], mesoporous carbon [5], carbon nanotubes [6], clay [7], carbon xerogel [8], and sodium alginate/graphene oxide composite beads [9].

Mesoporous carbons are good adsorbents because of their attractive features, such as a developed specific surface

area, high pore volume, tunable pore size, and good stability. Various approaches have been developed to prepare mesoporous carbons. A commonly used synthesis method is the template method, which may involve soft or hard templates. In the “hard-templating” route, mesoporous silica serves as a hard template, is impregnated with an appropriate carbon precursor, carbonized, and removed by treatment with NaOH or HF [10]. In the “soft-templating” route, a thermally decomposable polymer serves as the template. The mesoporous carbon is obtained by heating to degrade the sensitive copolymer molecules [11]. Recently, the use of multiple templating approaches to fabricate porous carbon materials with hierarchically porous structures and a designed porosity has received considerable attention. Huang et al. [12] used polystyrene latex spheres and triblock copolymer F127

\* Corresponding author.

as macro- and mesoporous structure-directing agents, with phenol–formaldehyde resin and Ni species as the carbon source and graphitization catalyst, respectively, to synthesize hierarchically porous carbon materials. The obtained product showed a high adsorption capacity for methylene blue.

The adsorption capacity depends on the pore structure of the carbon and functional groups on its pore surface. To enhance the adsorption capacity, post-treatment has often been applied, such as activation with CO<sub>2</sub> or functionalization of the carbon surface [5,13,14]. However, this complicates the preparation process. The aim of this study was to synthesize a mesoporous carbon for CIP removal by a simple double-template method. Nanosized silica and triblock copolymer F127 (EO<sub>106</sub>PO<sub>70</sub>EO<sub>106</sub>) were used as mesoporous structure-directing agents, and phenol–formaldehyde resin was added as a carbon precursor. The obtained mesoporous carbon was used to remove CIP from wastewater. CIP has been measured in water and wastewater from <1 µg/L to ~31 mg/L [15]. However, even at low concentrations, the presence of CIP can lead to the development of antibiotic-resistant bacteria. Therefore, adsorption tests were carried out at a low concentration. For comparison, other mesoporous carbon materials were prepared with only one template. The characteristics and adsorption properties of these mesoporous carbons and a commercial AC have been investigated.

The method developed herein has several advantages compared with previous techniques: (1) a simple preparation process; (2) the obtained mesoporous carbon has a large Brunauer–Emmett–Teller (BET) surface area and mesoporous volume; (3) the mesoporous carbon shows a high CIP adsorption, even at low analyte concentrations.

## 2. Materials and methods

### 2.1. Materials

The triblock copolymer Pluronic F127 was from Sigma-Aldrich (Shanghai, China). All other chemicals were of analytical grade from Beijing Chemistry Corporation (Beijing, China). All materials were used without further purification. Distilled water was purified by means of a Milli-Q water purification system (Millipore, Boston, USA). Novalac phenol–formaldehyde resin with hexamethylenetetramine (11 wt.%) was from Shandong Resin Industry (Shandong, China). The commercial AC was from Tongzhou Active Carbon Factory (Beijing, China).

### 2.2. Synthesis of mesoporous carbons

Novalac phenol–formaldehyde resin (2.5 g) with hexamethylenetetramine (11 wt.%) was dissolved in ethanol (10 mL) after which F127 (4 g) was added. After complete dissolution, mesoporous silica (4 g) was added. The mixture was heated at 100°C for 3 h. It was left to dry in air for 2 d and kept at 150°C for 1 h. The obtained composite was carbonized at 800°C for 2 h under nitrogen. The mesoporous silica template was removed by treatment with 40% HF solution. The obtained mesoporous carbon was washed thoroughly with distilled water and dried at 80°C overnight.

The mesoporous carbon is denoted MSF. MS and MF were synthesized in a similar manner, but with mesoporous silica (MS) or F127 (MF), respectively, as the sole template.

### 2.3. Characterization of mesoporous carbon

Nitrogen adsorption/desorption isotherms were measured at –196.15°C on a Micromeritics ASAP2020 analyzer. All samples were degassed at 110°C in a vacuum prior to the measurements. The surface area ( $S_{\text{BET}}$ ) was determined using the BET method. The total pore volume ( $V_t$ ) was calculated from the amount of nitrogen adsorbed at a relative pressure of 0.99. The micropore volume ( $V_{\text{micro}}$ ) was determined by the  $t$ -plot method. The mesoporous volume ( $V_{\text{meso}}$ ) was calculated as  $V_t - V_{\text{micro}}$ . Average pore sizes were estimated by the Barrett–Joyner–Halenda (BJH) method and pore size distributions were calculated from the desorption branches of isotherms using the same approach.

The point of zero charge ( $\text{pH}_{\text{PZC}}$ ) was determined according to a literature method [8]. The MSF was placed in 0.01 M NaCl solution (20 mL). The mixture pH was adjusted between 2 and 10 using 0.1 M HCl or 0.1 M NaOH solutions. The flasks were shaken for 20 h for the adsorption to reach equilibrium. A blank test was performed without a carbon sample to eliminate other influences. The mixture pHs were measured, and the  $\text{pH}_{\text{PZC}}$  was taken as the point at which the  $\text{pH}_{\text{initial}} - \text{pH}_{\text{final}}$  was zero.

### 2.4. Adsorption experiments

#### 2.4.1. Adsorption isotherms

In a typical adsorption experiment, identical portions (20 mg) of carbon adsorbent were added to conical flasks that contained CIP solutions (500 mL) of different concentrations. The flasks were capped and shaken at 25°C in a bath oscillator. The effects of CIP concentration and contact time were studied to investigate the CIP removal process. For the adsorption study, mixtures were shaken at pH 5.0. To investigate the effect of pH on adsorption, experiments were conducted at different pH from 3 to 11 at 25°C. The system pH was adjusted with 0.1 M NaOH or 0.1 M HCl solutions. CIP concentrations were determined spectrophotometrically at a maximum absorption wavelength of 275 nm [6]. A calibration curve was established with five standards between 0 and 20 mg/L, which gave a correlation coefficient  $R^2 > 0.999$ .

To model the adsorption behavior and to calculate the adsorption capacities of these carbon materials, adsorption isotherms were studied. Langmuir [16] and Freundlich isotherms [17] were examined for CIP adsorption. The respective models can be expressed by Eqs. (1) and (2):

$$\frac{C_e}{q_e} = \frac{1}{q_{\text{max}} K_L} + \frac{C_e}{q_{\text{max}}} \quad (1)$$

$$\ln q_e = \ln K_F + \frac{1}{n} \ln C_e \quad (2)$$

where  $C_e$  (mg/L) is the equilibrium concentration of the CIP,  $q_{\text{max}}$  (mg/g) is the maximum adsorption capacity of the adsorbent,  $K_L$  is a constant that is related to the adsorption

energy,  $q_e$  (mg/g) is the equilibrium adsorption capacity of the adsorbent,  $K_f$  is a constant that is related to the adsorption capacity of the adsorbent, and  $n$  is a constant that is related to the adsorption intensity.

2.4.2. Adsorption kinetics

The CIP adsorption kinetics on these carbon materials was studied at an initial concentration of 16.4 mg/L. Briefly, CIP solution (500 mL) and the adsorbent (20 mg) were stirred magnetically in a 1,000 mL flask. Aliquots (~3 mL) were withdrawn from the solution at different times and filtered prior to measuring the CIP concentrations. The results from these experiments were used to study the CIP adsorption kinetics. The CIP adsorption kinetics on these carbon materials was analyzed by using the pseudo-first-order and pseudo-second-order models [18].

The respective models can be expressed by Eqs. (3) and (4):

$$\log(q_e - q_t) = \log q_e - \frac{k_1}{2.303} t \tag{3}$$

$$\frac{t}{q_t} = \frac{1}{k_2 q_e^2} + \frac{1}{q_e} t \tag{4}$$

where  $k_1$  is the rate constant of the pseudo-first-order model and  $k_2$  is the rate constant of the pseudo-second-order model,  $q_t$  (mg/g) is the amount of CIP adsorbed at time  $t$ , and  $q_e$  (mg/g) is the adsorption capacity at equilibrium.

3. Results and discussion

3.1. Characterization of carbon materials

The nitrogen adsorption isotherms and the pore size distribution curves of MSF, MS, MF, and AC are shown in Fig. 1. For MSF and MS, the results indicate uniform, narrowly distributed mesopores and type-IV isotherms.  $H_1$  hysteresis

loops that are indicative of capillary condensation at relative pressures ( $P/P_0$ )  $\approx$  0.40–0.90 were observed. MF exhibited a mixed type-I and -IV isotherm according to the International Union of Pure and Applied Chemistry classification [2]. Such an isotherm is characteristic of materials that contain micropores and mesopores [19]. AC exhibited a type-I nitrogen adsorption isotherm, which is characteristic of a microporous adsorbent, as shown by its pore size distribution.

The BET surface areas, total pore volumes, mesopore volumes, micropore volumes, and average pore sizes of these carbon materials are summarized in Table 1. MSF has a high BET surface area (1,342.8 m<sup>2</sup>/g), total pore volume (1.406 cm<sup>3</sup>/g), and mesopore volume (1.365 cm<sup>3</sup>/g). The average pore size is ~4.19 nm. MS and MF have similar BET surface areas of 470.6 and 464.7 m<sup>2</sup>/g, total pore volumes of 0.665 and 0.259 cm<sup>3</sup>/g, and mesopore volumes of 0.602 and 0.122 cm<sup>3</sup>/g, respectively, which are lower than those of MSF. The average pore sizes of MS and MF are 5.60 and 2.23 nm, respectively. MF has a large amount of micropores, which results in smaller average pore size. The presence of micropores in MF may result from the collapse of pores during the degradation of F127 and expanding gases such as carbon dioxide and water vapor that are formed during carbonization at high temperatures. MSF maintains a high mesopore volume and a small micropore volume, probably because the mesoporous silica prevents pore collapse during the degradation of F127. AC contains micropores and the average pore size is 1.88 nm.

3.2. Adsorption of CIP

3.2.1. Adsorption isotherms

Fig. 2 shows the adsorption isotherms of CIP on the four-carbon samples. The MSF adsorption capacity is highest among the four adsorbents. The adsorption capacity decreased with a decrease in mesopore volume in the order MSF > MS > MF > AC. CIP has a molecular weight of 331 and a molecular length of 10.1 Å. However, a dimer of molecular length 14.4 Å may be produced, with a separation distance

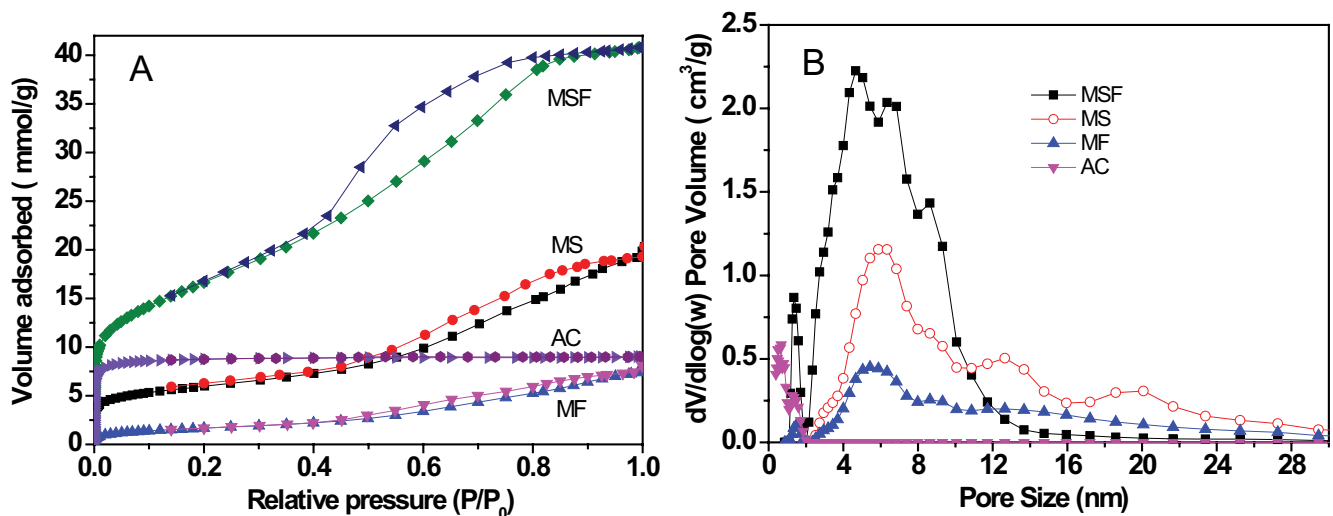


Fig. 1. (a) Nitrogen adsorption isotherms and (b) pore size distributions of MSF, MS, MF, and AC.

Table 1  
Physical properties and maximum CIP adsorption capacities of carbon adsorbents

Samples	$S_{\text{BET}}$ (m <sup>2</sup> /g)	$V_{\text{tal}}$ (cm <sup>3</sup> /g)	$V_{\text{meso}}$ (cm <sup>3</sup> /g)	$V_{\text{micro}}$ (cm <sup>3</sup> /g)	Average pore size (nm)	$q_{\text{max}}$ (mg/g)
MSF	1,342.8	1.406	1.365	0.041	4.19	243.91
MS	470.6	0.665	0.602	0.063	5.60	204.08
MF	464.7	0.259	0.122	0.137	2.23	190.84
AC	660.9	0.311	0.046	0.265	1.88	53.48
AC1	1,824.9	0.782	0.137	0.645	–	108.74 [20]
AC2	2,237	1.23	0.12	1.11	–	108.34 [21]
AC3	1,237	0.98	0.704	0.276	3.8	231.0 [22]

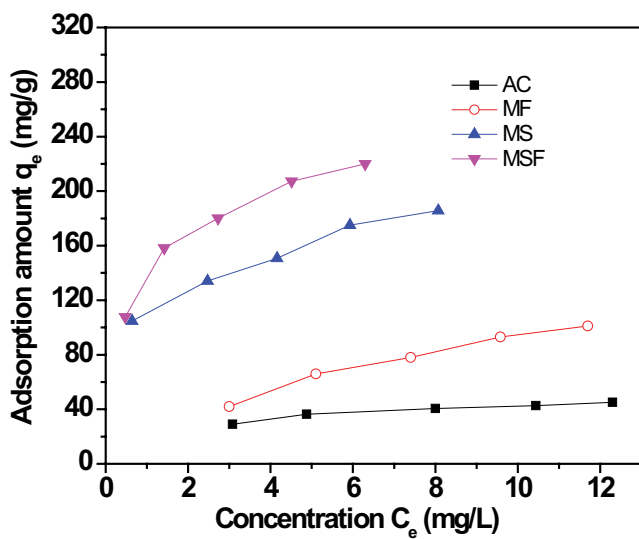


Fig. 2. CIP adsorption isotherms.

of 3.5–3.9 Å between the two molecules [4]. Therefore, CIP cannot enter micropores, and a high mesopore volume favors its adsorption.

In general, the surface area is a key factor that affects adsorption capacity. A large surface area will result in high adsorption capacity. However, in this study, although MS and MF had similar BET surface areas, the former showed a much higher adsorption capacity because of its higher mesopore volume. AC possesses mainly micropores, which do not allow the CIP molecule to penetrate. Therefore, AC showed the lowest adsorption capacity, even though its BET surface area is larger than those of MS and MF. The importance of the mesopores is indicated by literature data [20–22] (Table 1). AC1 and AC2 (Table 1) have high BET surface areas of 1,824.9 and 2,237 m<sup>2</sup>/g, total pore volumes of 0.782 and 1.23 cm<sup>3</sup>/g, and similar mesopore volumes of 0.137 and 0.12 cm<sup>3</sup>/g, respectively. They have a similar adsorption. The BET surface area of AC3 is smaller than that of AC1 and AC2. However, AC3 showed a higher adsorption capacity than AC1 and AC2 because of its higher mesopore volume. All results suggest that the mesopores are an effective space for CIP adsorption.

Adsorption isotherm models have been used extensively to investigate the adsorption and to elucidate their mechanisms. Adsorption equilibrium data for CIP were correlated

with the Langmuir (Eq. (1)) and Freundlich (Eq. (2)) models. The corresponding parameters, along with the correlation coefficients ( $R^2$ ), are given in Table 2. According to the correlation coefficients, the Langmuir and Freundlich isotherms fit the experimental data. However, the correlation coefficients showed that the Langmuir model better describes the adsorption equilibrium data. According to this model, the highest adsorption capacity of MSF was 243.91 mg/g.

Table 3 compares data for MSF with those of other CIP adsorbents in the literature. MSF had a higher adsorption capacity for CIP than the other materials at low concentrations of this analyte. Thus, MSF shows potential as an antibiotic adsorbent.

### 3.2.2. Adsorption kinetics

The adsorption kinetics of CIP was evaluated, and the results are shown in Fig. 3. For MSF and MS, the amounts adsorbed increased significantly in the first 5 h. Thereafter, a gradual increase was observed. The adsorption process reached equilibrium within 30 h, and no appreciable increase in adsorption was observed beyond this time. MF needed the longest time to reach equilibrium. MSF and MS have larger pores (Table 1), which lowers the diffusion resistance, such that CIP molecules can diffuse more easily in these adsorbents. MF has smaller pores (Table 1), and a longer time is needed to reach adsorption equilibrium because of the diffusion process that occurs therein. AC is composed mainly of micropores; adsorption occurs mainly on its surface because of the molecular sieving effect, hence the time to reach adsorption equilibrium is shorter than for MF.

To evaluate the adsorption kinetics, pseudo-first-order and pseudo-second-order models were studied. Kinetic parameters are listed in Table 4. According to the linear-regression correlation coefficients, the pseudo-second-order kinetic equation better described the adsorption of CIP on all carbon adsorbents with  $R^2 > 0.98$ . The amounts of CIP that were adsorbed experimentally were close to those implied by simulation, which supports the interpretation that CIP adsorption on carbon materials follows pseudo-second-order kinetics.

The above results show that MSF is an appropriate adsorbent for CIP, with a high adsorption capacity and a rapid adsorption rate. The adsorption capacity depends primarily on the pore structure properties of MSF and the molecular size of CIP. The solution pH also affects the adsorption capacity.

Table 2  
Parameters of Langmuir and Freundlich models of CIP adsorption on four carbon adsorbents

Samples	Langmuir			Freundlich		
	$q_{\max}$ (mg/g)	$K_L$ (L/mg)	$R$	$K_F$ (mg/g(L/mg) <sup>1/n</sup> )	$n$	$R$
AC	53.48	0.408	0.998	21.915	3.444	0.955
MF	190.84	0.097	0.979	21.744	1.566	0.978
MS	204.08	0.980	0.981	113.521	4.405	0.970
MSF	243.91	1.370	0.996	136.316	3.637	0.983

Table 3  
Maximum adsorption capacities of CIP on different adsorbents at a low CIP concentration

Adsorbents	Maximum adsorption amount (mg/g)	Refs.
Mesoporous carbon	243.9	This work
Activated carbon	108.7	[20]
Activated carbon	108.3	[21]
Activated carbon	231	[22]
Carbon xerogel	112	[22]
Carbon nanotubes	135	[22]
Kaolinite	6.3	[1]
Palygorskite-montmorillonite	0.107	[23]
Biocomposite fibers	66.25	[24]
Carbon nanofibers	225.3	[25]
Powder activated carbon	86.2	[25]
Carbon nanofibers	10.36	[26]

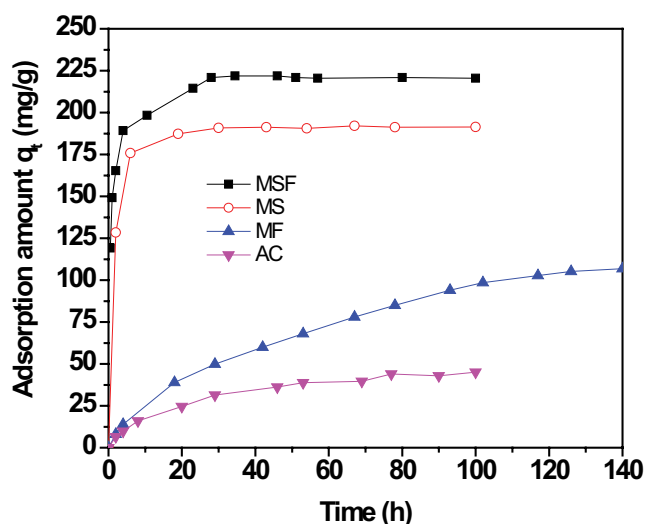


Fig. 3. Kinetic curves for CIP adsorption on the carbon adsorbents.

### 3.2.3. Adsorption mechanism

The effect of pH on the adsorption capacity of MSF was determined by using 21.13 mg/L aqueous CIP solutions at pH 3–11. As shown in Fig. 4, the adsorption capacity increased initially with pH, reached a maximum at pH 5–6, and then decreased at pH > 6.0. CIP exists as a positively

charged (cationic), negatively charged (anionic), and/or zwitterionic species at different pHs because of its different  $pK_a$  values (6.1 and 8.7). At a low pH, the positive CIP<sup>+</sup> species is present, and its percentage decreases continuously from pH 3 to pH 6.1. The  $pH_{PZC}$  of MSF is 4.9 (Fig. 4). The MSF surface is positively charged at pH <  $pH_{PZC}$  and negatively charged at pH >  $pH_{PZC}$  [27]. At pH < 4.9 and pH > 8.7, the MSF surface is of the same sign of charge as the CIP, which does not favor adsorption because of electrostatic repulsion. Increased electrostatic-induced adsorption can be expected at pH 4.9–6.1 because of the opposite charges of the CIP molecules and the MSF surface. In the pH range 6.1–8.7, CIP can exist as a zwitterionic or neutral species, and there is no significant electrostatic attraction or repulsion between the CIP and charged MSF surface. Hydrophobic interactions tend to be an important factor for driving organic compound adsorption on carbon adsorbents. The higher hydrophobicity of the zwitterionic CIP resulted in its greater adsorption at pH ≈ 7 [6]. However, a decrease in CIP adsorption on the MSF was observed in this pH range, which implies that hydrophobic interaction is not the main adsorption mechanism here. As expected, at pH > 8.7, the electrostatic repulsive interaction between MSF and CIP molecules became large, because the MSF surface and CIP remained negatively charged in aqueous solution, which decreased the amount adsorbed. Therefore, electrostatic interaction between CIP and MSF is a major factor that controls the adsorption, along with the MSF pore structure.

Table 4  
Kinetic parameters for CIP adsorption on carbon adsorbents

Sample	$q_e$ (mg/g) exp	Pseudo-first-order model			Pseudo-second-order model		
		$k_1$ (1/h)	$q_e$ (mg/g)	$R^2$	$k_2$ (1/g h)	$q_e$ (mg/g)	$R^2$
MSF	220	0.0496	21.252	0.391	$7.844 \times 10^{-3}$	222.717	0.999
MS	191	0.0557	26.862	0.629	$5.111 \times 10^{-3}$	196.078	0.999
MF	107	0.0282	129.018	0.925	$1.616 \times 10^{-4}$	138.122	0.981
AC	45	0.0364	41.725	0.918	$1.058 \times 10^{-3}$	52.083	0.993

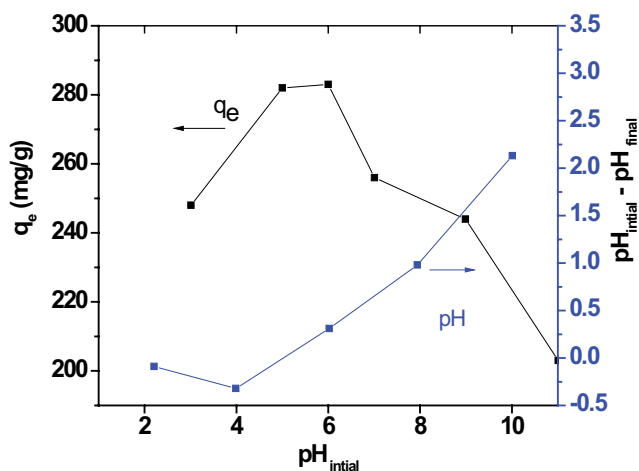


Fig. 4. Effect of pH on MSF adsorption capacity.

#### 4. Conclusions

A mesoporous carbon, MSF, was synthesized by a double-template method. This mesoporous carbon had a high BET surface area and a high mesopore volume. The adsorption capacity of MSF for CIP was larger than that of other adsorbents at a low CIP concentration, which showed it to be a good adsorbent for antibiotic contaminant removal. The adsorption capacity of MSF for CIP depends primarily on the mesopore volume. Electrostatic interaction between MSF and CIP influences the adsorption process. Therefore, MSF could be a promising adsorption material for CIP removal from water, especially at low analyte concentrations.

#### Acknowledgments

This work was supported by the Natural Science Foundation of China (No. 51772031).

#### References

- Z. Li, H. Hong, L. Liao, C.J. Ackley, L.A. Schulz, R.A. Macdonald, A.L. Mihelich, S.M. Emard, A mechanistic study of ciprofloxacin removal by kaolinite, *Colloids Surf., B*, 88 (2011) 339–344.
- K.S.W. Sing, Reporting physisorption data for gas/solid systems with special reference to the determination of surface area and porosity, *Pure Appl. Chem.*, 57 (1990) 603–619.
- Y. Sun, Q. Yue, B. Gao, Y. Gao, X. Xu, Q. Li, Y. Wang, Adsorption, and cosorption of ciprofloxacin and Ni(II) on activated carbon-mechanism study, *J. Taiwan Inst. Chem. Eng.*, 45 (2014) 681–688.
- Q. Wu, L. Tie, Z. Li, H. Hong, K. Yin, Adsorption and intercalation of ciprofloxacin on montmorillonite, *Appl. Clay Sci.*, 50 (2010) 204–211.
- X. Peng, F. Hu, L.Y. Lam, Y. Wang, Z. Liu, H. Dai, Adsorption behavior and mechanisms of ciprofloxacin from aqueous solution by ordered mesoporous carbon and bamboo-based carbon, *J. Colloid Interface Sci.*, 460 (2015) 349–360.
- H. Li, D. Zhang, X. Han, B. Xing, Adsorption of antibiotic ciprofloxacin on carbon nanotubes: pH dependence and thermodynamics, *Chemosphere*, 95 (2014) 150–155.
- C.J. Wang, Z. Li, W.T. Jiang, Adsorption of ciprofloxacin on 2:1 dioctahedral clay minerals, *Appl. Clay Sci.*, 53 (2011) 723–728.
- S.A.C. Carabineiro, T. Thavorn-Amornsri, M.F.R. Pereira, J.L. Figueiredo, Adsorption of ciprofloxacin on surface-modified carbon materials, *Water Res.*, 45 (2011) 4583–4591.
- Y. Fei, Y. Li, S. Han, J. Ma, Adsorptive removal of ciprofloxacin by sodium alginate/graphene oxide composite beads from aqueous solution, *J. Colloid Interface Sci.*, 484 (2016) 196–204.
- R. Ryoo, S.H. Joo, M. Kruk, M. Jaroniec, Ordered mesoporous carbons, *Adv. Mater.*, 13 (2001) 677–681.
- C. Liang, K. Hong, G.A. Guiochon, J.W. Mays, S. Dai, Synthesis of a large-scale highly ordered porous carbon film by self-assembly of block copolymers, *Angew. Chem. Int. Ed.*, 43 (2004) 5785–5789.
- C.H. Huang, R.A. Doong, D. Gu, D. Zhao, Dual-template synthesis of magnetically-separable hierarchically-ordered porous carbons by catalytic graphitization, *Carbon*, 49 (2011) 3055–3064.
- F. Liu, Z. Guo, S. Zheng, Z. Xu, Adsorption of tannic acid and phenol on mesoporous carbon activated by CO<sub>2</sub>, *Chem. Eng. J.*, 183 (2012) 244–252.
- Z. Guo, G. Zhu, B. Gao, D. Zhang, G. Tian, Y. Chen, W. Zhang, S. Qiu, Adsorption of vitamin B12 on ordered mesoporous carbons coated with PMMA, *Carbon*, 43 (2005) 2344–2351.
- N. Carosini, L.S. Lee, Ciprofloxacin sorption by dissolved organic carbon from reference and bio-waste materials, *Chemosphere*, 77 (2009) 813–820.
- R.L. Tseng, F.C. Wu, R.S. Juang, Liquid-phase adsorption of dyes and phenols using pinewood-based activated carbons, *Carbon*, 41 (2003) 487–495.
- Z. Aksu, E. Balibek, Chromium(VI) biosorption by dried *Rhizopus arrhizus*: effect of salt (NaCl) concentration on equilibrium and kinetic parameters, *J. Hazard. Mater.*, 145 (2007) 210–220.
- D.K. Mahmoud, M.A.M. Salleh, A.W.A.K. Wan, A. Idris, Z.Z. Abidin, Batch adsorption of basic dye using acid-treated kenaf fiber char: equilibrium, kinetic and thermodynamic studies, *Chem. Eng. J.*, 181–182 (2012) 449–457.
- G.S. Miguel, G.D. Fowler, M.D. Orso, C.J. Sollars, Porosity and surface characteristics of activated carbons produced from waste tyre rubber, *J. Chem. Technol. Biotechnol.*, 77 (2002) 1–8.
- M.J. Ahmed, S.K. Theydan, Fluoroquinolones antibiotics adsorption onto microporous activated carbon from lignocellulosic biomass by microwave pyrolysis, *J. Taiwan Inst. Chem. Eng.*, 45 (2014) 219–226.
- Y.X. Wang, H.H. Ngo, W.S. Guo, Preparation of a specific bamboo-based activated carbon and its application for ciprofloxacin removal, *Sci. Total Environ.*, 533 (2015) 32–39.

- [22] S.A.C. Carabineiro, T. Thavorn-amornsri, M.F.R. Pereira, P. Serp, J.L. Figueiredo, Comparison between activated carbon, carbon xerogel and carbon nanotubes for the adsorption of the antibiotic ciprofloxacin, *Catal. Today*, 186 (2012) 29–34.
- [23] T.M. Berhane, J. Levy, M.P.S. Krekeler, N.D. Danielson, Adsorption of bisphenol A and ciprofloxacin by palygorskite-montmorillonite: effect of granule size, solution chemistry and temperature, *Appl. Clay Sci.*, 132–133 (2016) 518–527.
- [24] S. Wu, X. Zhao, Y. Li, C. Zhao, Q. Du, J. Sun, Y. Wang, X. Peng, Y. Xia, Z. Wang, Adsorption of ciprofloxacin onto biocomposite fibers of graphene oxide/calcium alginate, *Chem. Eng. J.*, 230 (2013) 389–395.
- [25] X. Li, S. Chen, X. Fan, X. Quan, F. Tan, Y. Zhang, J. Gao, Adsorption of ciprofloxacin, bisphenol and 2-chlorophenol on electrospun carbon nanofibers: in comparison with powder activated carbon, *J. Colloid Interface Sci.*, 447 (2015) 120–127.
- [26] X. Peng, F. Hu, J. Huang, Y. Wang, H. Dai, Z. Liu, Preparation of a graphitic ordered mesoporous carbon and its application in sorption of ciprofloxacin: kinetics, isotherm, adsorption mechanisms studies, *Microporous Mesoporous Mater.*, 228 (2016) 196–206.
- [27] Z. Wang, X. Yu, B. Pan, B. Xing, Norfloxacin sorption and its thermodynamics on surface-modified carbon nanotubes, *Environ. Sci. Technol.*, 44 (2010) 978–984.